JOURNAL OF MAGNETIC RESONANCE IMAGING 20:555–562 (2004)

Original Research

Diffusion Tensor Eigenvector Directional Color Imaging Patterns in the Evaluation of Cerebral White Matter Tracts Altered by Tumor

Aaron S. Field, MD, PhD,[1]* Andrew L. Alexander, PhD,[2,3] Yu-Chien Wu, MD,[2] Khader M. Hasan, PhD,[2] Brian Witwer, MD,[4] and Behnam Badie, MD[4]

Purpose: To categorize the varied appearances of tumor-altered white matter (WM) tracts on diffusion tensor eigenvector directional color maps.

Materials and Methods: Diffusion tensor imaging (DTI) was obtained preoperatively in 13 patients with brain tumors ranging from benign to high-grade malignant, including primary and metastatic lesions, and maps of apparent diffusion coefficient (ADC), fractional anisotropy (FA), and major eigenvector direction were generated. Regions of interest (ROIs) were drawn within identifiable WM tracts affected by tumor, avoiding grossly cystic and necrotic regions, known fiber crossings, and gray matter. Patterns of WM tract alteration were categorized on the basis of qualitative analysis of directional color maps and correlation analysis of ADC and FA.

Results: Four basic patterns of WM alteration were identified: 1) normal or nearly normal FA and ADC, with abnormal tract location or tensor directions attributable to bulk mass displacement, 2) moderately decreased FA and increased ADC with normal tract locations and tensor directions, 3) moderately decreased FA and increased ADC with abnormal tensor directions, and 4) near isotropy. FA and ADC were inversely correlated for Patterns 1–3 but did not discriminate edema from infiltrating tumor. However, in the absence of mass displacement, infiltrating tumor was found to produce tensor directional changes that were not observed with vasogenic edema, suggesting the possibility of discrimination on the basis of directional statistics.

Conclusion: Tumor alteration of WM tracts tends to produce one of four patterns on FA and directional color maps. Clinical application of these patterns must await further study.

Key Words: diffusion tensor imaging; clinical applications; cerebral neoplasms; directional encoding; preoperative planning
J. Magn. Reson. Imaging 2004;20:555–562.

MAPPING OF WHITE MATTER (WM) tracts through magnetic resonance (MR) measurements of the water diffusion tensor may allow the relationship of a tumor to functional, connective pathways to be assessed preoperatively. Recent studies (1–7) suggest that this method holds great promise, but there are several technical challenges that remain to be solved before it will gain widespread clinical use in neurosurgical patients. Much of the early work on diffusion tensor imaging (DTI) of WM tracts has (appropriately) focused on the normal brain; DTI of pathologic WM tracts is still in its infancy and it remains to be seen how useful tract mapping will be in various pathologic states.

A cerebral neoplasm may alter the state of WM in several ways, at either the gross anatomic or cellular level. For example, some neoplasms might displace WM fiber tracts as they enlarge, altering the position or orientation of the fibers while leaving them intact. Other neoplasms might infiltrate WM tracts by insinuating themselves between individual fibers without disrupting their directional organization, or else might simply destroy them outright. These alterations may manifest at some distance beyond the margins of a tumor, owing to the potential for Wallerian degeneration. Vasogenic edema surrounding a neoplasm also can infiltrate WM tracts and might be expected to do so without altering their orientation. Complicating the situation is the fact that any or all of these altered states may coexist in the same region.

The altered states of WM resulting from cerebral neoplasm might be expected to influence the measurement of diffusion tensor anisotropy and orientation in various ways. Intact WM tracts displaced by tumor might

[1]Department of Radiology, University of Wisconsin Medical School, Madison, Wisconsin.
[2]Department of Medical Physics, University of Wisconsin Medical School, Madison, Wisconsin.
[3]Department of Psychiatry, University of Wisconsin Medical School, Madison, Wisconsin.
[4]Department of Neurological Surgery, University of Wisconsin Medical School, Madison, Wisconsin.
Contract grant sponsor: NIH; Contract grant number: R01 EB 002012.
Presented in part at ISMRM Workshop on Diffusion MRI Biophysical Issues, St. Malo, France, March 10–12, 2002.
*Address reprint requests to: A.S.F., Assistant Professor of Radiology, University of Wisconsin Medical School, E3/311 Clinical Science Center, 600 Highland Avenue, Madison, WI 53792-3252.
E-mail: as.field@hosp.wisc.edu
Received November 26, 2003; Accepted June 23, 2004.
DOI 10.1002/jmri.20169
Published online in Wiley InterScience (www.interscience.wiley.com).

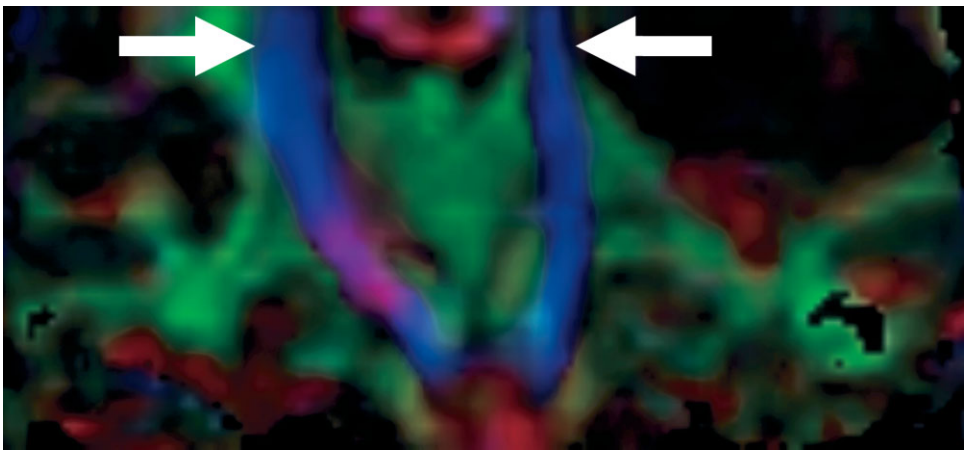

Figure 1. Example of DTI Pattern 1 (normal anisotropy, abnormal location): coronal directional color map showing corona radiata (blue voxels, arrows) displaced medially by a grade-III astrocytoma in the left frontal lobe.

retain their anisotropy and remain identifiable in their new location or orientation on directional maps (1–7). Conversely, infiltrated WM tracts might lose some anisotropy but retain their directional organization and orientation, remaining identifiable in their normal location on directional maps (4,6,7). Of course, WM tracts might be destroyed or disrupted to the point where directional organization (and, consequently, diffusion anisotropy) is lost completely.

The behavior of DTI and directional mapping methods under these conditions has not been well characterized to date, and their clinical utility in preoperative planning is unclear. With this in mind we evaluated our DTI and directional mapping techniques on a series of brain tumor patients undergoing preoperative MR imaging, and report our experience herein. We have attempted to categorize the varied appearances of tumor-altered WM tracts to aid in future radiologic interpretations of these maps.

MATERIALS AND METHODS

Thirteen patients, ranging in age from 20 to 66 years (mean 43 years), with intracranial neoplasms were included in the study under Institutional Review Board approval. Pathologic diagnoses were obtained within one to two weeks of imaging in all patients and included four oligodendrogliomas (World Health Organization Classification grade II), three solitary metastases (one each of melanoma, adenocarcinoma, and squamous cell carcinoma), two anaplastic astrocytomas, and one each of the following: glioblastoma multiforme, malignant oligoastrocytoma, pilocytic astrocytoma, and ganglioglioma. All tumors were limited to one cerebral hemisphere.

MR imaging was done at 1.5 T on a GE (Waukesha, WI) CVi Signa scanner using a standard quadrature birdcage head coil. In addition to routine clinical imaging sequences, a single-shot spin-echo echo planar imaging (EPI) pulse sequence (4500/71.8 msec TR/TE, number of excitations [NEX] 4, 240 mm field of view [FOV], 3-mm slice thickness) with diffusion weighting was used to obtain diffusion-tensor encoded images. Images were obtained with 23 diffusion-tensor encoding directions, which were generated with a minimum energy optimization algorithm that distributed the directions uniformly over a unit sphere to minimize directional biases (8). Diffusion weighting of b = 1000 sec/mm^2 was used and a single reference image without diffusion weighting (b $\sim$ 0) was obtained. The EPI acquisition matrix was 128 $\times$ 128, which was zero-filled to 256 $\times$ 256. The acquisition was done in two slabs of 20 slices each because of image-number limitations on the scanner. The top slab covered from the vertex to the midbrain, and the bottom slab from the midbrain to the brainstem. Each slab required 7 minutes 30 seconds to acquire (15 minutes total scan time).

Image misregistration from motion and eddy current distortion was corrected using a two-dimensional image registration algorithm (eight parameter model) in automated image registration (AIR) (9). The two diffusion tensor slabs were combined into a single three-dimensional volume. One common overlapping slice between the two slabs was used to ensure good coregistration between the two slab volumes. A 3 $\times$ 3 median filter was applied to each diffusion-weighted image to improve the image signal-to-noise ratio; although this was achieved at the expense of some blurring of tract boundaries, differences in anisotropy values between filtered and unfiltered maps did not exceed 0.02, and the blurring was considered tolerable for present purposes. The combined single volume slab was interpolated to isotropic voxel dimensions (0.94 $\times$ 0.94 $\times$ 0.94 mm^3). Tensor decoding was then performed on the 23 diffusion-encoded images (post-registration, filtering, and interpolation) to estimate the diffusion tensor for each location in the image volume (10). The diffusion tensor information was then represented by maps of apparent diffusion coefficient (ADC = trace/3), fractional anisotropy (FA), and major eigenvector direction. Directional maps were generated by mapping the major eigenvector components into red, green, and blue color channels, with color brightness modulated by FA.

For qualitative analysis, a certificate of added qualification (CAQ)-certified neuroradiologist with working knowledge of fiber tract anatomy viewed ADC, FA, and

directional color maps to determine which tracts in the tumor vicinity were visibly abnormal on any of these maps. The location of each tract and its hue on directional color maps were classified as normal or abnormal, based on comparison to the homologous tracts in the contralateral hemisphere, which were unaffected by tumor in all cases. For quantitative analysis, regions of interest (ROIs) were manually drawn on the directional color maps by the radiologist and copied to ADC maps. ROIs were limited to recognizable WM fiber tracts in the vicinity of the tumor, taking care to avoid gray matter and regions of obvious cyst formation, necrosis, or fiber crossings. A total of 23 ROIs were drawn, encompassing 21,522 0.83-mm^3 voxels (approximately 17.9 cc of tissue). Similarly sized ROIs were then drawn in homologous tracts in the contralateral hemisphere. Mean ADC and FA were calculated over all voxels within each ROI and the correlation coefficient between ADC and FA was calculated over all ROIs. Processing was performed using algorithms and display tools developed in IDL (Research Systems, Boulder, Colorado).

In order to characterize the DTI pattern of vasogenic edema, we examined the ADC, FA, and directional data for the three metastasis cases, each of which featured a solitary, small and focal, metastatic lesion producing no substantial mass effects and surrounded by a much larger region of peritumoral WM edema that could reasonably be presumed tumor-free. A total of six ROIs, encompassing a total of 5,054 0.83-mm^3 voxels (approximately 4.2 cc of tissue), were drawn in these cases. As a preliminary attempt to distinguish infiltrating tumor from vasogenic edema on the basis of DTI patterns, we compared the ADC, FA, and directional data from the metastasis cases to those from two infiltrating gliomas (grade II oligodendroglioma and anaplastic astrocytoma).

Finally, DTI was performed postoperatively on three patients and the directional color maps were qualitatively compared against their preoperative counterparts to assess the extent to which peritumoral WM tracts were altered by resection of tumor.

RESULTS

The directional color maps with FA incorporated by way of color intensity modulation provided a concise, readily interpretable summary of the anisotropic diffusion characteristics of tumor-altered WM fiber tracts and revealed four basic DTI patterns.

Fiber tracts showing Pattern 1 were characterized by normal or mildly decreased FA (<25%) and normal or mildly increased ADC (<25%) relative to the homologous tract in contralateral hemisphere, with abnormal location and/or direction resulting from bulk mass displacement (Fig. 1). Patterns 2 and 3 both were characterized by substantially decreased FA and increased ADC but differed in their appearance on directional color maps. Whereas Pattern-2 tracts were normal in location and direction (i.e., showed normal color hues), Pattern-3 tracts exhibited abnormal hues not attributable to bulk mass displacement. Pattern 2 was observed in peritumoral WM tracts that showed probable vasogenic edema without tumor (the solitary metasta-

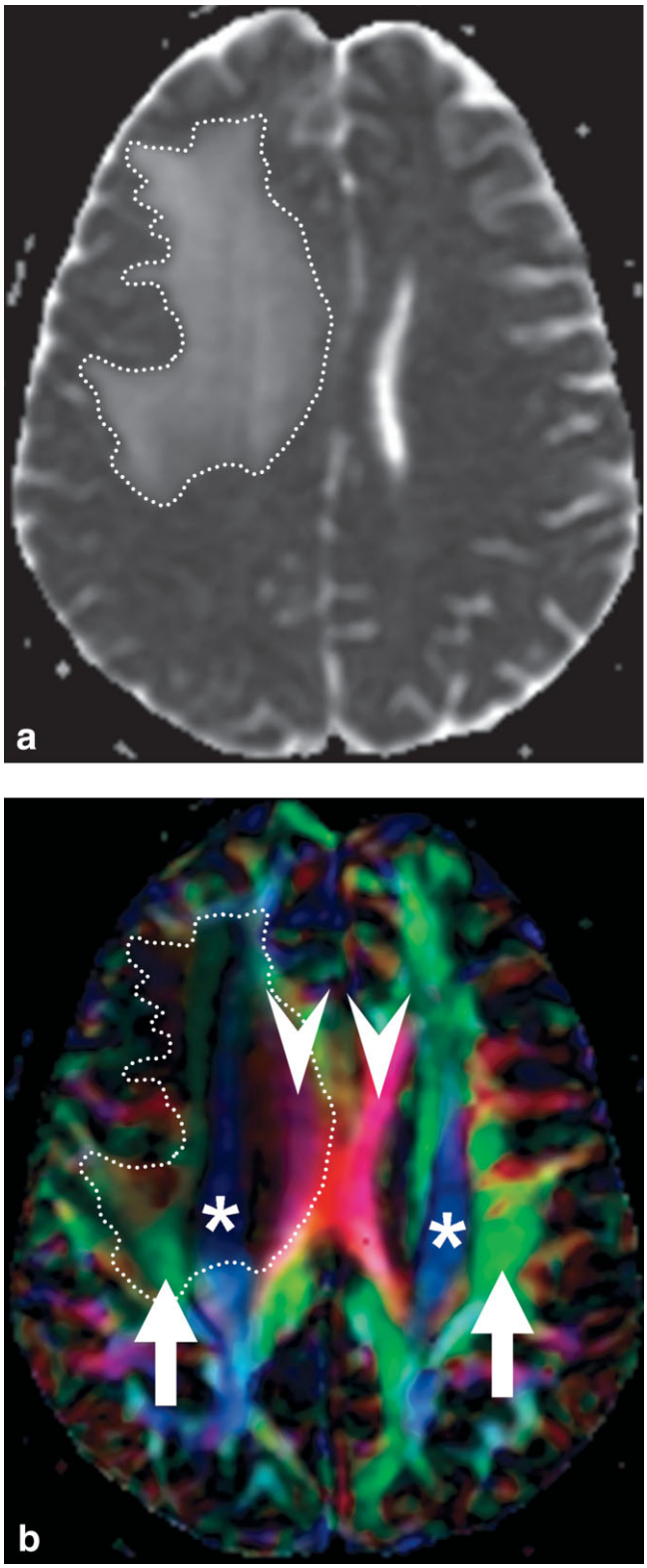

Figure 2. Example of DTI Pattern 2 (decreased anisotropy, normal location/orientation). **a:** ADC map showing increased diffusivity in region of vasogenic edema (outlined) involving right corona radiata (CR), arcuate fasciculus (AF), and corpus callosum (CC). **b:** Directional color map showing reduced anisotropy (reflected by diminished color brightness) in CR (blue, asterisks), AF (green, arrows), and CC (red, arrowheads) but with normal location and orientation of these tracts (reflected by normal hues compared to homologous tracts in contralateral hemisphere).

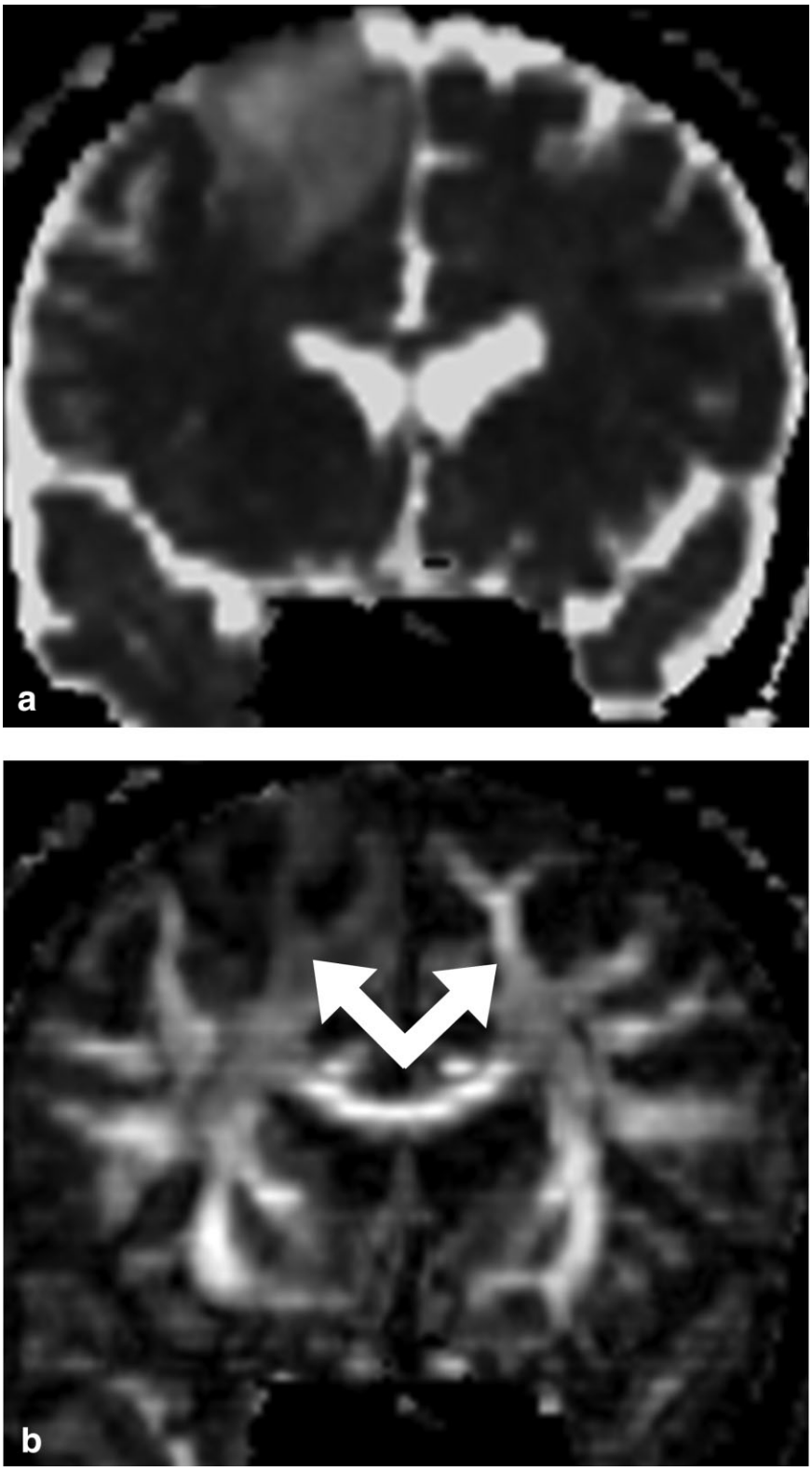

Figure 3. Example of DTI Pattern 3 (reduced anisotropy, disorientation without significant mass displacement). **a:** Coronal ADC map showing increased diffusivity in a diffusely infiltrating, grade-II oligodendroglioma of the right frontal lobe. FA (**b**) and directional color maps (**c**) corresponding to ADC map, showing both reduced anisotropy and disorientation of WM fibers (reflected in asymmetric color hues) resulting from this tumor (arrows). Compare the predominantly inferior-superior oriented (blue) fibers in the (normal) left hemisphere to the predominantly anterior-posterior oriented (green) fibers in the tumor (arrows).

ses, Fig. 2), but was also seen in other cases where the absence of tumor could not be assumed. Pattern 3 was observed only in the two infiltrating gliomas (Fig. 3). In some cases a combination of Patterns 1 and 2 was found, with tracts showing both bulk mass displacement and infiltration by either tumor or edema (Fig. 4). Pattern 4 was characterized by isotropic or near-isotropic diffusion, such that the tract was not identifiable on FA or directional color maps (Fig. 5).

Patterns 1, 2, and (1+2) combined were identified in both benign and malignant tumors. Pattern 3 was limited to the infiltrating gliomas, but there were only two of these. Pattern 4 was limited to malignant tumors, but was seen in both high- and low-grade malignancies.

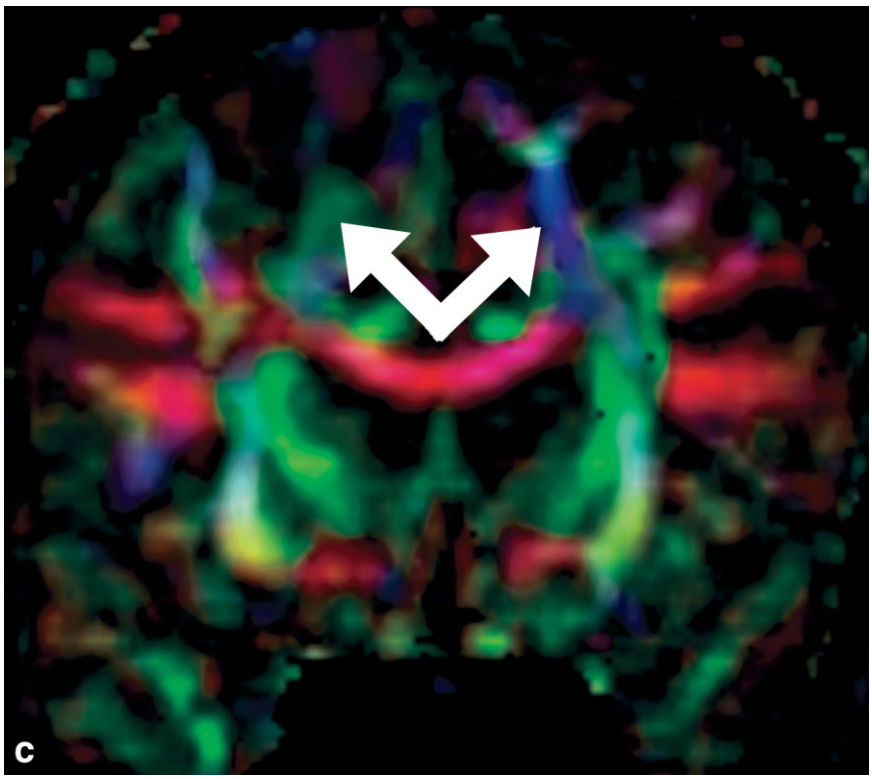

Figure 3 (Continued)

There was a significant inverse relationship between FA and ADC for Patterns 1–3 (Fig. 6). Because ROIs were limited to identifiable WM tracts, Pattern 4 was not included in this calculation.

All of the ROIs drawn in regions of vasogenic edema surrounding small metastases (no bulk mass displacements) showed Pattern 2 (Fig. 2). ADC and FA for these ROIs (four cases, seven total ROIs) were $1203 \pm 147 \times 10^{-6}$ mm^2/second and 0.22 ± 0.02, respectively (mean ± SD). Relative to their homologous contralateral ROIs, these values were +67% (SD 19%) and –49% (SD 11%), respectively. As noted above, the two infiltrating tumors showed DTI Pattern 3 (Fig. 3).

Postoperative directional color maps obtained in three patients demonstrated preservation, and return to anatomic position, of WM fiber tracts that were displaced by tumor on preoperative maps (Fig. 7). Preservation of these tracts was facilitated by the preoperative mapping.

DISCUSSION

Applications of diffusion MR in the evaluation of cerebral neoplasms have generally focused on measurements of mean diffusivity and/or anisotropy in various tumor components or peritumoral tracts (11–21). There have been very few prior studies in which the full diffusion tensor, replete with information on the directional organization of WM fiber tracts, has been exploited for the purpose of characterizing the structural alterations of specific tracts in the region of a neoplasm (1–7).

WM tracts may be pathologically altered by tumor in several ways; specifically, they may be displaced, infiltrated by tumor and/or edema, or destroyed. We identified four imaging patterns that presumably reflected these alterations on FA-weighted directional color maps, and we presented examples of each herein. Unfortunately, however, these alterations are not mutually exclusive in a given tumor or even in a given WM tract, and no simple correspondence between the pathology and the imaging patterns was found. This may be due, at least in part, to the markedly heterogeneous nature of many CNS neoplasms, which makes the drawing of appropriate ROIs inherently difficult and highly subjective. Moreover, different tracts may respond differently in the face of a given variety of tumor growth; we do not yet have sufficient experience to attribute any particular behavior to any specific tract. Neither do we have sufficient pathologic data to correlate with DTI findings. The collection of such data is limited by practical constraints; for example, it is not ethically possible to biopsy areas presumed to represent bland edema, nor is it possible to biopsy a tract that appears to be merely displaced in order to confirm that it is not infiltrated also.

We made every effort to limit ROIs to WM tracts that were altered by the presence of tumor while remaining identifiable, based on the author's knowledge of WM tract anatomy and comparisons of FA and directional color maps between hemispheres ipsilateral and contralateral to the tumor. Known tracts that could not be identified were assumed destroyed. Of course, no accounting for tracts that may have been altered beyond recognition, yet still preserved, is possible with this approach. While it would not completely eliminate this problem, a less subjective approach would be enabled by a normal DTI template constructed from a series of coregistered FA and directional color maps obtained from a large, normal pop-

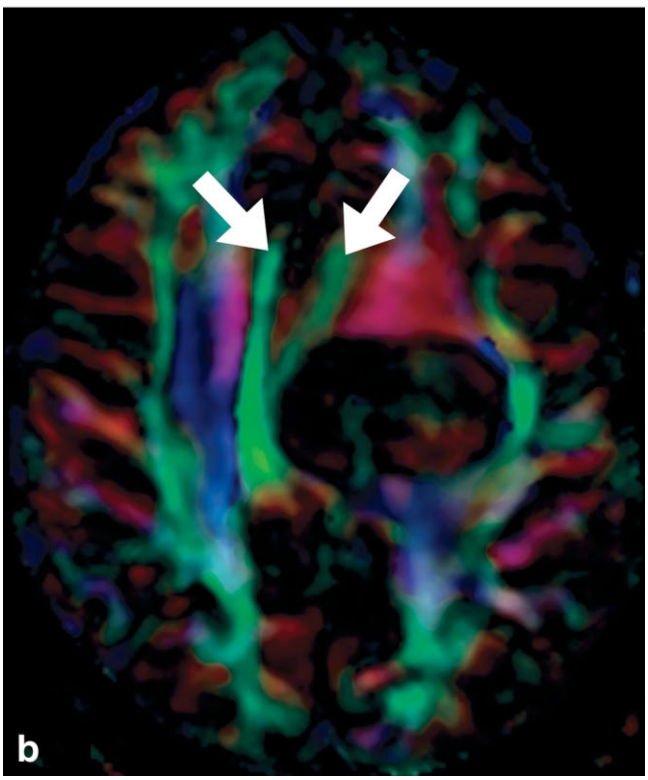

Figure 4. Example of combination DTI Patterns 1 and 2 (reduced anisotropy, displacement to abnormal location). **a:** ADC map showing increased diffusivity in edematous or infiltrated left cingulum (arrow), surrounding a grade-III astrocytoma. **b:** Directional color map showing left cingulum (arrow) to have both reduced anisotropy (reflected by diminished green color intensity) and abnormal location (displaced medially). Cingula indicated by arrows.

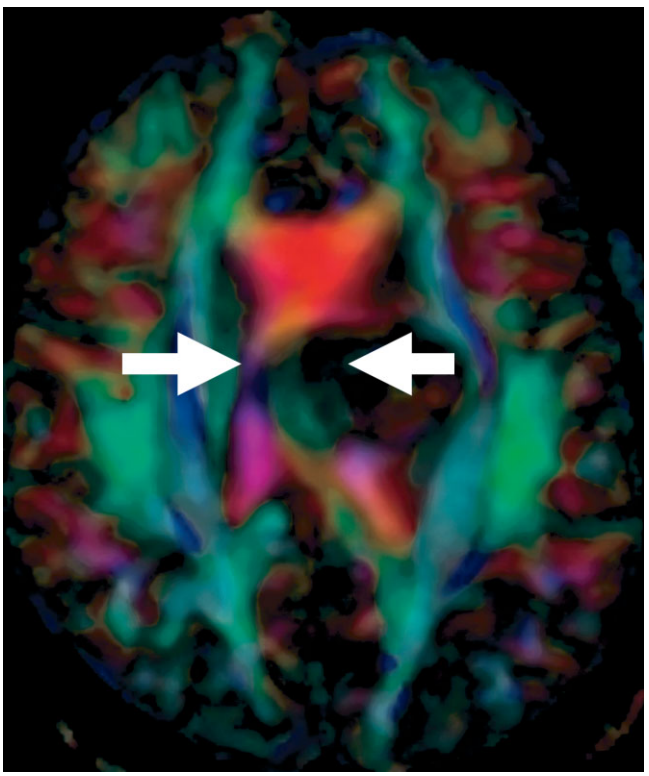

Figure 5. Example of DTI Pattern 4 (complete destruction, no residual anisotropy, tract no longer identifiable). This directional color map shows complete destruction of the body of the corpus callosum (arrows) by a grade-III astrocytoma.

ulation. Such a template is not yet available but efforts to develop such a template are underway by several research groups, including our own.

The preoperative depiction of a tumor's relationships to WM tracts using DTI and directional color mapping proved to be extremely useful to the neurosurgeons in this

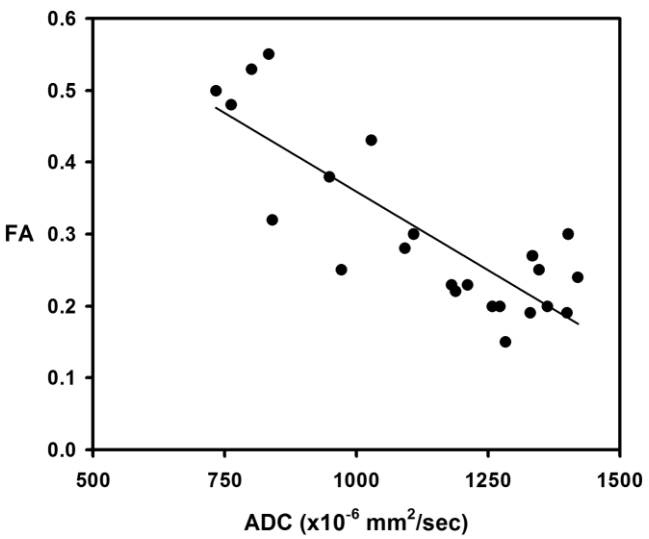

Figure 6. FA vs. ADC for DTI Patterns 1–3. (Pattern 4 tracts excluded because these were unidentifiable by definition.) Absolute values are inversely correlated (R = 0.81).

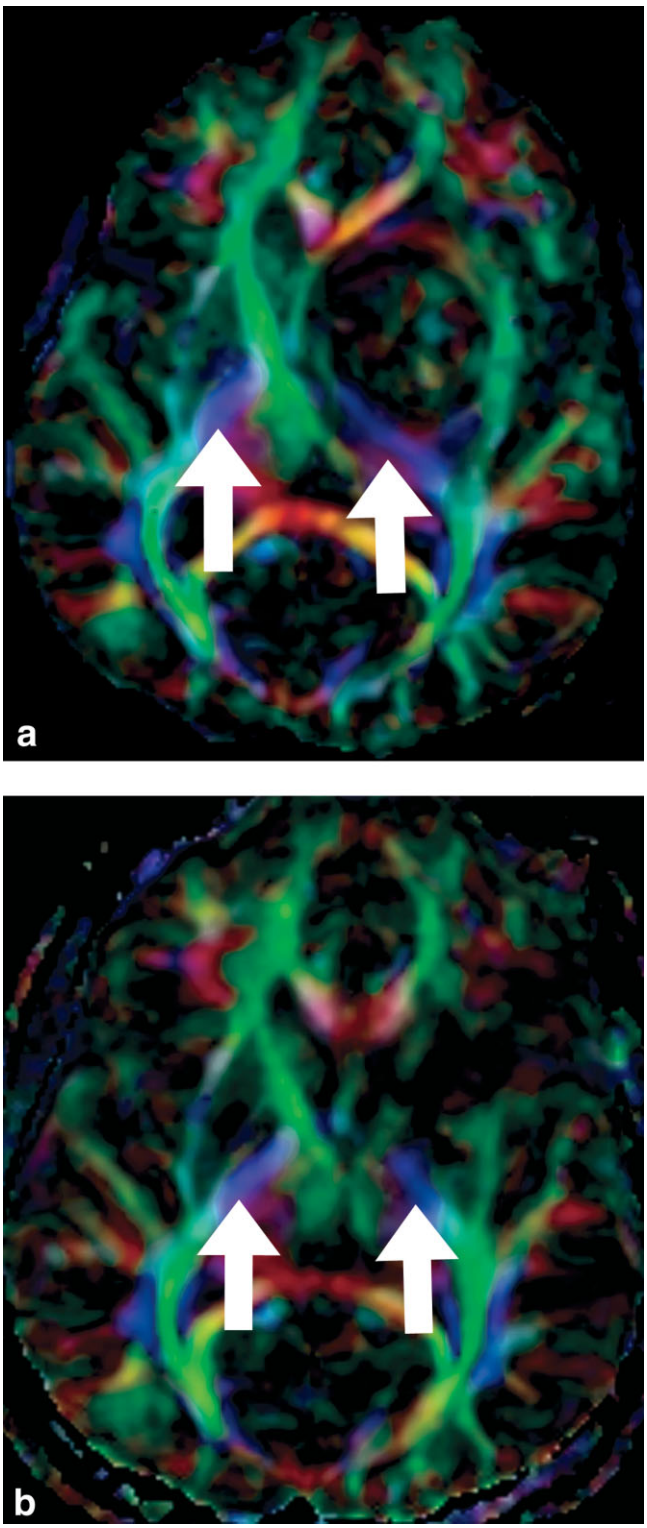

Figure 7. a: Preoperative directional color map shows posteromedial displacement of the left corticospinal tract by a pilocytic astrocytoma (DTI Pattern 1). **b:** Postoperative map shows this tract has been preserved and returned to near-anatomic position following tumor resection.

series of patients. For example, knowing that a WM tract was intact but displaced by tumor to a new location (Pattern 1) allowed the surgeon to adapt his approach to preserve this tract during resection. Similarly, knowing that specific WM tracts were destroyed by tumor (Pattern 4) allowed the surgeon to attempt gross total resection without undue concern for preserving these tracts or risking new functional deficits postoperatively. Neurosurgeons at the authors' institution now obtain preoperative DTI routinely for any tumors thought to potentially involve critical WM fiber tracts.

As noted above, the patterns most useful to preoperative planning were Patterns 1 and 4. Perhaps more interesting are Patterns 2 and 3, which appear to be associated with the infiltration of WM tracts by tumor and/or edema. The effects of vasogenic edema on the diffusion tensor, coupled with the frequent observation of vasogenic edema in the vicinity of cerebral neoplasms, has important implications for peritumoral tissue characterization and fiber tracking by DTI. In particular, the discrimination of "bland" edema (tumor-free) from infiltrating tumor—both of which exhibit T2-hyperintensity, increased ADC, and decreased FA—is as challenging as it is important. Previous studies have addressed this problem through the analysis of ADC and FA values, with mixed results (11–21). The present study must be counted among those that were unable to discriminate tumor from edema on the basis of ADC and FA alone. However, we have taken an additional step by analyzing the directional color maps, and our preliminary results are encouraging if not definitive. We found that vasogenic edema in the absence of bulk mass displacement tends to exhibit reduced FA without associated directional changes, as reflected by normal hues on directional color maps (Pattern 2). Contrast this with our findings in two cases of infiltrating tumor, where the FA reduction was accompanied by a more severe form of disorganization reflected in abnormal hues on directional color maps. There did not appear to be sufficient bulk mass displacement to account for these changes, but the explanation for this pattern currently remains speculative. One possibility in these cases is that one of two differently-oriented sets of fibers in close proximity normally "dominates" the diffusion tensor and tumor infiltration of the dominant fibers effectively "unmasks" another set of fibers to result in altered color hues. This is worthy of more quantitative study through the application of directional statistical analysis (22,23).

In conclusion, the alteration of WM tracts by tumor produced one or more of four distinct patterns on DTI with directional color mapping. No simple correspondence between tumor type or grade and imaging pattern was observed. Correlations between pathology and imaging pattern must await further studies with DTI and biopsy data co-localized to the extent possible. Directional mapping provides more complete tissue characterization than do mean diffusivity and diffusion anisotropy alone, and should be exploited more quantitatively in future studies through the use of directional statistical techniques.

REFERENCES

1. Wieshmann UC, Symms MR, Parker GJM, et al. Diffusion tensor imaging demonstrates deviation of fibres in normal appearing white matter adjacent to a brain tumour. J Neurol Neurosurg Psychiatry 2000;68:501–503.

2. Holodny AI, Schwartz TH, Ollenschleger M, Liu W-C, Schulder M. Tumor involvement of the corticospinal tract: diffusion magnetic resonance tractography with intraoperative correlation[case illustration]. J Neurosurg 2001;95:1082.
3. Holodny AI, Ollenschleger MD, Liu WC, Schulder M, Kalnin AJ. Identification of the corticospinal tracts achieved using blood-oxygen-level-dependent and diffusion functional MR imaging in patients with brain tumors. AJNR Am J Neuroradiol 2001;22:83–88.
4. Mori S, Frederiksen K, van Zijl PCM, et al. Brain white matter anatomy of tumor patients evaluated with diffusion tensor imaging. Ann Neurol 2002;51:377–380.
5. Clark CA, Barrick TR, Murphy MM, Bell BA. White matter fiber tracking in patients with space-occupying lesions of the brain: a new technique for neurosurgical planning? Neuroimage 2003;20: 1601–1608.
6. Witwer BP, Moftakhar R, Hasan KM, et al. Diffusion tensor imaging of white matter tracts in patients with cerebral neoplasm. J Neurosurg 2002;97:568–575.
7. Field AS, Alexander AL, Hasan KM, et al. Diffusion tensor MR imaging patterns in white matter tracts altered by neoplasm. Presented at ISMRM Workshop on Diffusion MRI Biophysical Issues, St. Malo, France; March 10–12, 2002. p 137–140.
8. Hasan KM, Parker DL, Alexander AL. Comparison of gradient encoding schemes for diffusion-tensor MRI. J Magn Reson Imaging 2001;13:769–780.
9. Woods RP, Cherry SR, Mazziotta JC. Rapid automated algorithm for aligning and reslicing PET images. J Comput Assist Tomogr 1992; 16:620–633.
10. Hasan KM, Basser PJ, Parker DL, Alexander AL. Analytical computation of the eigenvalues and eigenvectors in DT-MRI. J Magn Reson 2001;152:41–47.
11. Guavain KM, McKinstry RC, Mukherjee P, et al. Evaluating pediatric brain tumor cellularity with diffusion-tensor imaging. AJR Am J Roentgenol 2001;177:449–454.
12. Guo AC, Cummings TJ, Dash RC, Provenzale JM. Lymphomas and high-grade astrocytomas: comparison of water diffusibility and histologic characteristics. Radiology 2002;224:177–183.
13. Tien RD, Felsberg GJ, Friedman H, Brown M, MacFall J. MR imaging of high-grade cerebral gliomas: value of diffusion-weighted echoplanar pulse sequences. AJR Am J Roentgenol 1994;162:671–677.
14. Brunberg JA, Chenevert TL, McKeever PE, et al. In vivo MR determination of water diffusion coefficients and diffusion anisotropy: correlation with structural alteration in gliomas of the cerebral hemispheres. AJNR Am J Neuroradiol 1995;16:361–371.
15. Lu S, Ahn D, Johnson G, Cha S. Peritumoral diffusion tensor imaging of high-grade gliomas and metastatic brain tumors. AJNR Am J Neuroradiol 2003;24:937–941.
16. Castillo M, Smith JK, Kwock L, Wilber K. Apparent diffusion coefficients in the evaluation of high-grade cerebral gliomas. AJNR Am J Neuroradiol 2001;22:60–64.
17. Stadnik TW, Chaskis C, Michotte A, et al. Diffusion-weighted MR imaging of intracerebral masses: comparison with conventional MR imaging and histologic findings. AJNR Am J Neuroradiol 2001;22: 969–976.
18. Kono K, Inoue Y, Nakayama K, et al. The role of diffusion-weighted imaging in patients with brain tumors. AJNR Am J Neuroradiol 2001;22:1081–1088.
19. Sinha S, Bastin ME, Whittle IR, Wardlaw JM. Diffusion tensor MR imaging of high-grade cerebral gliomas. AJNR Am J Neuroradiol 2002;23:520–527.
20. Krabbe K, Gideon P, Wagn P, Hansen U, Thomsen C, Madsen F. MR diffusion imaging of human intracranial tumours. Neuroradiology 1997;39:483–489.
21. Bastin ME, Sinha S, Whittle IR, Wardlaw JM. Measurements of water diffusion and T1 values in peritumoral oedematous brain. Neuroreport 2002;13:1335–1340.
22. Wu Y-C, Field AS, Badie B, Alexander AL. Quantitative analysis of diffusion tensor eigenvectors of white matter infiltration by tumors and edema. In: Proceedings of the 11th Annual Meeting of ISMRM, Toronto, Canada, 2003.
23. Wu Y-C, Field AS, Chung MK, Badie B, Alexander AL. Quantitative analysis of diffusion tensor orientation: theoretical framework. Magn Reson Med 2004; in press.